

We are IntechOpen, the world's leading publisher of Open Access books Built by scientists, for scientists

6,900

Open access books available

186,000

International authors and editors

200M

Downloads

Our authors are among the

154

Countries delivered to

TOP 1%

most cited scientists

12.2%

Contributors from top 500 universities



WEB OF SCIENCE™

Selection of our books indexed in the Book Citation Index
in Web of Science™ Core Collection (BKCI)

Interested in publishing with us?
Contact book.department@intechopen.com

Numbers displayed above are based on latest data collected.
For more information visit www.intechopen.com



Advanced Train Positioning/Communication System

Fouzia Elbahhar and Marc Heddebaut

Additional information is available at the end of the chapter

<http://dx.doi.org/10.5772/intechopen.71768>

Abstract

In the past, in order to ensure train positioning as well as ground-to-train information exchange, railways have adopted various technologies. Over time, each new generation of equipment enriched the global information exchange but, as a consequence, necessitated higher data rate transfers. For the positioning functionality, the existing localisation systems are still limited, since most of them require an infrastructure installation with constraints such as laying equipment between the rails or having high database maintenance requirements and computational costs. Moreover, some of them accumulate errors (odometers and inertial sensors) or offer limited coverage in shadowed areas (GNSS, etc.). Currently, in railway applications, a widely used localization system is based on proprioceptive sensors embarked in the train. This on-board system is coupled to the use of balises located at ground between the rails. These balises are kilometre markers. They are used to compensate for the drift of the localization information computed using the proprioceptive sensors alone, when the train moves. The balises provide absolute localization information whenever the train passes over them. They can also provide spot communication during the short period of time when trains are passing over them. In the first part of this chapter, techniques for achieving train positioning and data exchanges between trains and infrastructure are introduced. In the second part, a new balise is proposed. Particular attention is paid to the contribution of this new solution in terms of localization error and communication performances.

Keywords: railway balise, MISO-UWB, time reversal technique, localization error, physical layer performances

1. Introduction

This chapter is organised in two main parts. Sections 1–7 present railway requirements in terms of train tele-positioning and self-positioning systems. It also describes some corresponding generic technical solutions. Moreover, in Sections 5 and 6, the document focuses on the use of

railway balises installed along the track. They are exploited for train positioning, as well as spot ground-to-train communications. Current existing technologies for these balises are then recalled, and potential technical limitations are deduced. In the second part of the chapter, in Section 8, a new balise using the Ultra-Wideband Impulse-Radio (UWB-IR) technique associated to the Time Reversal (TR) technique is introduced and extensively analysed. Then, Section 9 presents some experimental results characterising the operation of this balise. Finally, Section 10 draws a conclusion.

2. Train speed control

During the 1970s, a number of railway accidents came to recall that the safety of rail transport was not strictly guaranteed, and that there were, in particular but not only, some technical gaps to be filled. Accidents continued to occur in the 1980s, and experts noticed that stop signals, normally leading to the mandatory shutdown of trains, were often not respected by train drivers. These studies convinced railway operators that the operation of trains based solely on human control was not sufficient to ensure the desired level of safety for this mode of transport. It was therefore necessary to envisage the introduction of a speed control system that would complement and control the supervision carried out by drivers and, if necessary, imposed on them.

An effective train speed control requires access to several parameters. A vital parameter requires constant knowledge of the geographical location of all trains, also known as train positioning, circulating along the railway network. Train positioning, combined with train identification, as well as the knowledge of the characteristics of the track, makes it possible to generate, from a distant ground operator, speed instructions transmitted to the train, ranging from full speed allowed at this point of the railway network to an absolute stop. This allows safe circulation of all the trains circulating along the railway line. Of course, the safety requirements associated with the development of such a speed control and particularly train positioning of the trains arise are extremely high. Consequently, it imposes significant repercussions on the technologies likely to be used to ensure this technical function.

3. Safety integrity levels

Since in railway operation the lives of human beings are at stake, safety is of major concern for train speed control and therefore train positioning. In particular, dangerous failure modes must be reduced to an extremely low level. In railway operation, as in many other industrial operations, safety integrity levels (SILs) are used to determine the necessary target level of risk reduction. The IEC 61508 standard defines four SILs that correspond to different probability of failure per hour [1]. SIL 4 corresponds to the more critical situations and the lowest probability of failure per hour.

A SIL is determined using a number of quantitative factors that are combined with qualitative factors including hardware safety integrity and systematic safety integrity. As a consequence, SIL 4 must be achieved for speed control and for any train positioning hardware.

On the ground side, two major technologies are currently operational on most of the world's rail networks. They are based, on the one hand, on the use of track circuits and, on the other hand, on track balises providing positioning and ground-to-train spot radio communication. On the train side, an odometry processing unit exploiting different sensor technologies is used. Merging different technologies helps reducing common mode failures, as SIL 4 certification is mandatory for this equipment.

4. Track circuit, a safe train tele-positioning system

The track circuit is one of the very first electrical signalling systems used to ensure the safety of rail traffic. It makes it possible to detect the presence of at least one train present on a length of railway track called a fixed block and indirectly to ensure a safe distance between the trains running on the same line. Some also allow the transmission of speed and stop instructions to the train. Although its principle is very old, different manufacturers have developed many distinct technical achievements. Track circuit current use is almost universal on railway networks [2]. The general principle of operation of the track circuit is as follows: the track is physically divided into several fixed blocks from a few hundred metres to a few kilometres long. The length depends on the use of the line and the speeds of the trains circulating there. A signal, the characteristics of which are related to the type of track circuit used (frequency and amplitude), is emitted along the rails by a transmitter placed at one end of the block. If the receiver at the other end receives this signal, then the fixed block is declared unoccupied. This information is reported to the ground train speed control system. In the opposite case, if the train is located somewhere along the fixed block, the signal does not reach the receiver because the two rails are short-circuited by the axle of the train and the fixed block is declared occupied. This positioning information is determined from the ground, not by the train itself, e.g. tele-positioning, and reported to the distant ground-based train speed control system.

We notice that, for these track circuits, the two rails are used as a bifilar untwisted transmission line. Due to the use of steel rails directly placed on the ground, on ballast, this transmission line presents rapidly increasing losses, as the frequency increases. In practice, only low frequencies, up to a few kHz (1–2 kHz), make it possible to obtain communication ranges compatible with fixed block lengths up to 2–3 km [3].

From the point of view of train safety operation, it is therefore mandatory to detect the presence of effective trains on all the occupied fixed blocks and to be certain that these trains actually occupy the detected cantons, but not other fixed blocks. Depending on the type of separation used between the different fixed blocks, many types of track circuits exist based on the same general principle, but exploiting different technical approaches, not interoperable between them. In practice, separation between fixed blocks may be carried out by an insulating joint, which physically separates the various sections of the rails. With welded rails, low frequency, e.g. audio frequencies (AF) at 1–2 kHz can be used. An electrical joint based on a set of parallel inductances and capacitors acts as a filter preventing the passage of the low frequency signal from a fixed block to the following one. **Figure 1** presents such a filter used in a so-called UM71 AF jointless track circuit [4].

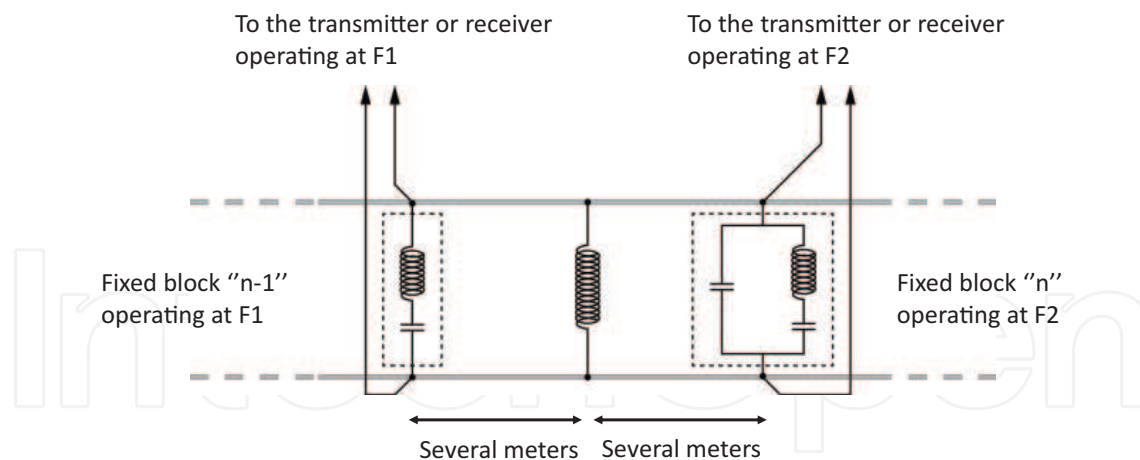


Figure 1. Filtering low frequency signals between two consecutive fixed blocks.

Fixed block noted $n - 1$ is travelled by a low-frequency $F1$ signal, which is heavily attenuated while passing through the filter and therefore almost undetectable in the following fixed block noted n . In the same way, fixed block n is travelled by a signal at frequency $F2$, which is also heavily attenuated while passing through the filter, so to be undetectable in the preceding fixed block $n - 1$. Therefore, all the consecutive fixed blocks can exploit the same alternation of frequencies $F1$ and $F2$. Frequencies $F1$ and $F2$ are chosen sufficiently low to enable a sufficient communication range and outside of potential harmonic signals coming from the electric train traction energy. They also must be sufficiently different to be effectively filtered. Of course, industrial choices can differ a bit, and technically, track circuits can be implemented differently from one network to another one, which also raises the problem of railway interoperability between different networks.

We deduce that track circuits provide a safe train detection of all the trains circulating along the railway level, with a spatial resolution limited to the length of the fixed block. Moreover, if the identification of the train is known by other technical means, then train tele-positioning, of course not very accurate since train positioning is only known somewhere along the fixed block, but safe, is provided.

5. Train odometry and balises

On the train side, measurements of the speed and position to deduce train self-positioning are continuously determined using an odometer exploiting different proprioceptive sensors. These sensors may consist of axle counters; they determine speed and covered distance knowing the circumference of the wheel [5]. To measure the speed and distance covered another way, microwave Doppler radars pointed to the ballast may also be used [6]. These Doppler radars exploit back scattering from the ballast, and their frequency can be optimised for the particular granulometry of the used ballast. **Figure 2** illustrates these two widely used sensor families.

Inertial sensors and global navigation satellite system (GNSS) sensors, among others are also used, are considered.

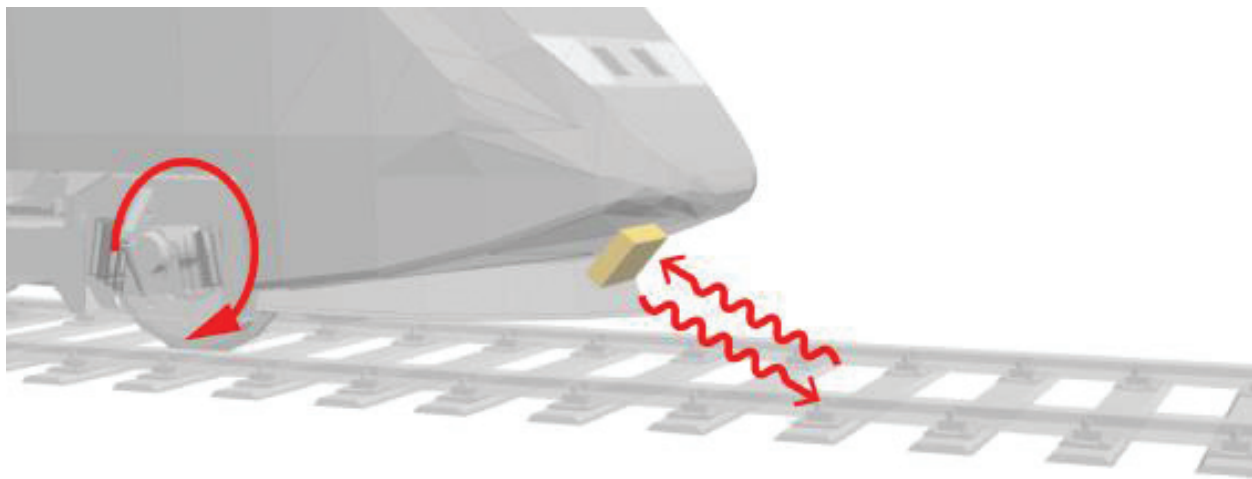


Figure 2. Proprioceptive sensors to feed the train odometer.

A measurement uncertainty and a progressive drift of the positioning accuracy are usually associated with each of these sensors. For example, due to wear, the circumference of the wheel is not perfectly stable and therefore not known perfectly. Consequently, over time, an increasing drift characterises the axle counter measurement. On its side, the Doppler measurement can be almost fully cancelled if water or wet snow lies between the rails. Indeed, this reduces or cancels the retro-diffusion effect. During the movement of the train, this results in temporary losses of information that affect the output information. Also, due to the low Doppler frequency generated, Doppler radars have limitations to measure very low speed, this drawback does not affect wheel counters. Considering these two sensor families, we verify that the use of very different sensor technologies helps to reduce common mode errors in order to build a global SIL 4 odometer.

Sensor drifts are compensated for balises regularly secured on the sleepers of the track. **Figure 3** shows such a balise installed between the rails. The trains embark a balise interrogator and reader located under the train body.



Figure 3. Example of balise mounted on the track.

These balises act as kilometre markers. They deliver to the passing trains their absolute positioning along the track. These data locally cancel the accumulated train odometer drift. After passing a balise, the train odometer restarts computing speed and position up to the next balise located on the track, at a distant where the accumulated drift is not yet problematic. These balises are also used in automated guided transport, for example, in order to calculate a precise station stop and to obtain the opening of the doors of the train exactly in front of the landing doors of stations.

These balises are often one of the latest, or even the latest, the last pieces of electronic equipment located at a very exposed and critical place, between the rails, on the track.

6. Speed control using balises

As described in the preceding section, balises are used as kilometre markers. They are installed regularly along the track, at accurately known locations, so that passing trains can read their absolute location on the fly. Moreover, these balises are also used to exchange data using spot ground-to-train radio communication. Balise-based speed control systems are installed in many railway networks. They provide automatic control of the speed and override of certain closed stop signals. In order to do this, the system uses a calculator on board the locomotives. The calculator takes into account both the information characterising the mobile and the data characterising the track and the location of the signals in order to determine a speed control curve that cannot be exceeded. This integrates the reaction time of each train equipment. Data are transmitted from the ground to the train through the balises. When a critical speed is reached, the train driver human machine interface sends an audible signal to warn the human operator of the need for urgent operation on his part to bring the speed back to a value acceptable to the system. If this action of the driver is not carried out quickly, the system will automatically stop the train by irreversible emergency braking, until it fully stops. The driver must then request from the ground controller a new driving authorization, after this total shutdown.

7. Current balise technology example

In Europe, balises are produced by a group of seven industrial companies: Alstom, Ansaldo STS, Bombardier, Invensys, Siemens, Sigma-Digitek and Thales, united within UNIFE, a federation of suppliers of railway equipment. This industrial grouping has defined and standardised eurobalise specifications and the associated test specification. The development of these specifications is driven by the European Railway Agency [7].

In the principle currently in play by eurobalises, the trains remotely power these beacons by magnetic coupling from a high-frequency 27 MHz, high-power signal emitted from an interrogator/beacon reader located under the train. These signals are emitted constantly as soon as the train is moving.

The magnetic coupling technology used by these balises was selected during the work carried out in the European project EURET 1.2, which was completed and published in 1996. Original Ericsson equipment, already a mature technology at that time, was compared to other techniques and has been selected and optimised in order to give the current eurobalise.

Benefits include interoperability over all the EU railway networks and efficient operation. Concerning the disadvantages, in addition to the electromagnetic pollution generated by the high power almost constant use of the train transmitter, it will be noted that this is the last indispensable equipment located at the track between the rails, which can generate constraints, in particular during the maintenance operations of the track. It is also an old analog technology, well below the current state of the art, using congested frequency bands and capable of generating and suffering electromagnetic disturbances in the vicinity.

A solution using satellite tracking techniques for trains is currently considered by several teams, but the requirements of railway signalling in terms of safety and reliability are strong and constraints linked to the physics of the problem leave room for doubt as to the emergence of a purely SIL 4 satellite-based track positioning solution for railway signalling. In particular, this is due to the wide disparity of environments likely to be encountered by trains in circulation.

8. Balises emerging technologies

Recently, railway balises have received renewed attention. Techniques considering state-of-the-art solutions rather than the old, currently used ones are being studied. In [6], fast-moving Radio Frequency IDentification (RFID) tags are studied in high-speed railway systems. However, authors identify issues, such as collision and insufficient reading time, and propose various ways to alleviate their effect in railway systems. Moreover, these new balises would remain located between the rails on the track. This proves to be constraining from the point of view of maintenance of the track, when it is necessary to add new ballast or to change rails, for examples.

A new generation balise using modern, energy-efficient, and green technologies is proposed in the following of this chapter. This balise is designed to operate from the side of the track and uses the ultra-wideband impulse radio (UWB-IR) radio technique. This technique possesses the intrinsic qualities of having a short-range, high communication capacity, of requiring low emitted power while providing precise relative location capability. Moreover, UWB technique has a low signal intercept capability by non-accredited users. Thus, there are strong arguments in favour of a future SIL 4 certification for a railway balise based on this technique.

This UWB pulse technique uses non-sinusoidal signals and transmits pulses of very short duration. They occupy an extended spectrum of at least 500 MHz bandwidth. Transmitters are of simple design and low consumption. These UWB transmissions are authorised worldwide in a specific power gauge [8]. Associated with the UWB-IR radio technique, a time reversal (TR) technique is also used [9]. The TR technique makes it possible to spatially and temporally focus an electromagnetic signal in a dispersive propagation medium. The principle

of the TR of the waves is based on the invariance of the equation of propagation of waves by reversal of time. This invariance allows a wave to backtrack so that it can replay the “go” scene of its propagation but backwards. The operating principle of this new generation balise is presented in **Figure 4**. The conventional balise situated between the rails is removed and replaced by the new balise, installed on a pole, on the side of the track and a few meters away. This new balise focuses the radiofrequency energy coming from the pole transmitters to an area situated over the rails, right over the removed conventional balise location. Therefore, this new balise does not interfere anymore with track maintenance operations but still develops a maximum of radio frequency signal at this particular location over the rails. Several transmitters are coupled on the pole; three can be seen in **Figure 4** to get a multiple source transmitter. This insures transmitter redundancy as well as space focusing when correctly configured. One single receiver or train-balise reader is used located in front of the train. This configuration is usually denoted as a Multiple Input, three transmitters, Single Output, one receiver, MISO 3×1 system.

Table 1 establishes a comparison of performance between the communication and localization systems using a railway conventional balise “existing balise” and the expected performance of the presented TR-UWB balise.

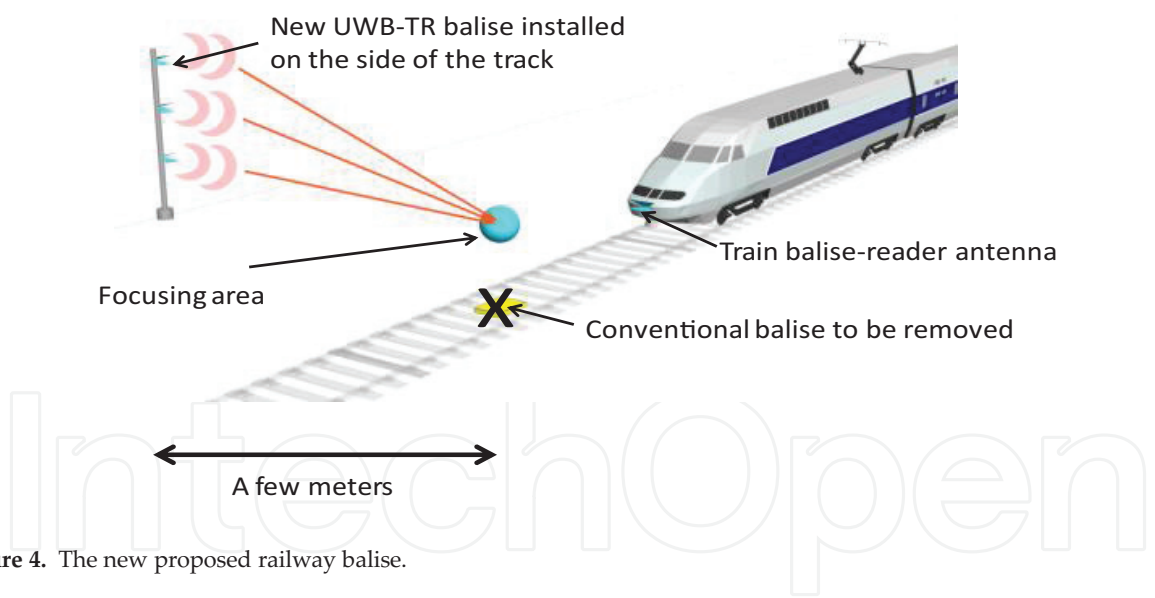


Figure 4. The new proposed railway balise.

	Conventional balise	TR-UWB balise
Operating frequency	27.095 MHz train to ground 4.5 MHz ground to train	3.1–10 GHz
Communication range	<1 m	10–100 m
Transmission rates	560 kbps	Potentially up to several hundred Mbps
Localization accuracy expected	20 cm	<10 cm

Table 1. Performance comparison between a conventional balise and the proposed balise.

8.1. Ultra-wideband radio technique

The UWB technology involves the transmission of very short pulses, typically having a time duration of 1 ns or less, therefore occupying a very wide frequency spectrum [10]. The use of this technology for our proposal is motivated by the following reasons:

- its potentially high transmission data rate, thanks to the very large frequency bandwidth used,
- its high resolution train location due to its very fine temporal resolution,
- its availability and robustness to multipath tunnel because of the large frequency bandwidth used,
- its low probability of detection due to a very low transmitted power; this property is necessary for safe and secure operation of the railway system,
- its ability to coexist with other radio systems thanks to low power spectral densities that do not require allocating a specific frequency band.

These reasons make UWB a novel, effective and complete solution for communication and localization in railways applications. Therefore, regulation bodies have considered the use of UWB in railway applications. **Table 2** provides some inputs regarding areas of operation of UWB systems [8].

However, the channel propagation effects, especially the lack of line of sight (LOS) between the transmitter and the receiver, and the presence of strong multipath are two significant sources of error for the localisation function. The introduction of UWB in wireless communication has brought improvements regarding these sources of errors [8]. Concerning the UWB technique, previous investigations have raised major issues, such as the complexity of the signal processing

Frequency (GHz)	Area of operation	Critical factors impairing system performance	Countermeasures compatible with limits and regulations
3.11 < f < 4.8 PSD < -53.3 dBm/MHz for unregistered UWB unlicensed mobile devices with 5% activity LDC PSD < -41.3 dBm/MHz for registered devices	Very short range (<10 m) short range (<50 m)	Multipath Broadband interferers (e.g. automotive UWB) Multipath + path loss Broadband interferers	Multiple UWB emitters onboard the train cars real-time processing Multiple "ground-based". fixed receivers Multiple UWB emitters at 3.1–4.8 GHz deployed as "ground-based" fixed references for real-time processing
6 < f ≤ 8.5 PSD < -53.3 dBm/MHz for unregistered UWB mobile devices with 5% LDC	Very short range (<10 m)	Multipath	Multiple UWB emitters onboard the train cars. Real-time processing. Narrow-beam antenna

Note: At highest frequencies (6 < f ≤ 8.5 GHz) very short-range (<10 m) applications only are affordable, due to the fact that fixed infrastructures made of UWB emitters are not allowed by the Electronic Communications Committee (ECC).

Table 2. Critical factors limiting the performance of UWB systems in railway environments.

at the reception [11, 12]. Therefore, UWB has been associated with TR [13, 14], especially in multi-users communication systems, in order to solve part of these problems and to report some of the noted complexity at the transmitter level.

8.2. Time reversal

Time reversal (TR) has been applied to acoustics and underwater systems [15]. It is closely related to the retro-directive array in microwave [16] and phase conjugation in optics. The first TR experiment using electromagnetic waves in the 2.45 GHz band was reported in [17]. This contribution suggests that the techniques developed for ultrasound might also be used for the study of electromagnetic case. It is an interesting challenge because in many real environments (buildings or cities), microwaves, using wavelengths between 5 and 30 cm, are scattered off by objects such as walls, desks, vehicles, and so on, which produces a multitude of paths from the transmitter to the receiver.

In such situation, a TR system should be able not only to compensate for the multipath effect but should also improve radio communication parameters, thanks to the many existing reflections/reverberations.

TR has two main characteristics, the temporal focusing and the spatial focusing; these are very beneficial to the UWB system [17, 18]. More recently, TR has also been studied for broadband radio communications, especially for UWB radio [13].

For our proposed TR-UWB system, we selected the second Gaussian derivative function as the signal shape to transmit [15]. Then, the channel impulse response (CIR) is measured between the transmitter (Tx) and the receiver (Rx), and the channel state information is loaded into Tx. The selected signal and the impulse response are then reversed in time and transmitted by Tx in the propagation channel, up to Rx. This process, represented in **Figure 5**, can be mathematically described by noting $s(t)$ the transmitted pulse, $h(t)$ the complex impulse response of the channel and $h^*(-t)$ the complex conjugate of the time reversed version of $h(t)$; $y(t)$ the received signal without TR and $y_{RT}(t)$, the received signal with TR at the receiver; one has:

$$\begin{aligned} y(t) &= s(t) \otimes h(t) + n(t) \\ y_{RT}(t) &= s(t) \otimes h^*(-t) \otimes h(t) + n(t) \\ h_{eq}(t) &= h^*(-t) \otimes h(t) \end{aligned}$$

Applied to our proposed railway balise, this TR general process becomes the following one. The local Channel State Information (CSI) between each balise transmitter and the distant area, where the energy must be focused is measured or computed a single time during the installation phase of the balise. Moreover, as trains will support the embarked balise reader, the CSI measurement is performed in presence of a metallic reflective mask representing the front of a train. It is situated at the distant area considered between the rails, where a maximum anticipated focusing effect is expected. This unique CSI is then loaded in the transmitter equipment to perform the TR operation. As long as the propagation environment remains unmodified, this initial CSI can be repetitively used by the balise. This information is then introduced as

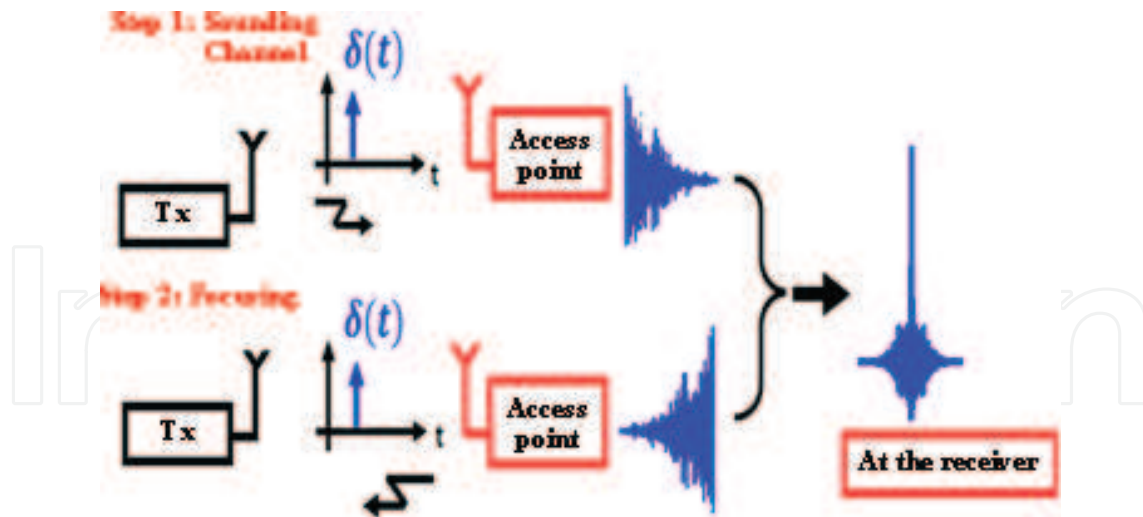


Figure 5. Principle of time reversal technique.

pre-filtering data in the different balise transmitters. Therefore, focusing is obtained in the required position, along the track, potentially improving the absolute localization process [14]. Moreover, using a single balise, focusing can be achieved successively toward different tracks, therefore, addressing different trains and delivering specific data to each train.

8.2.1. Parameters to evaluate TR effectiveness

The autocorrelation function is used to evaluate the temporal focusing (TF) and the spatial focusing (SF). To study TF, one can evaluate the Focusing Gain (FG), which is defined as the ratio of the spectrum power of strongest amplitude peak in TR received to the strongest peak received by a conventional UWB system. The focusing gain can be written as:

$$FG_{[dB]} = 20 \log_{10} \left(\frac{\max(|y_{tr}(t)|)}{\max(|y(t)|)} \right) \quad (1)$$

Higher FG usually translates into higher communication range and higher precision of localization for a localization system as compared to a classical system.

The study of SF considering a simple transmitter to receiver configuration is performed the following way. The channel impulse response (CIR) of the intended receiver located in position p_0 is noted $h(p_0, t)$. The CIR of the unintended receiver located in position $p_{i(i \neq 0)}$ is noted $h(p_i, i \neq 0)$. The equivalent CIR of the intended receiver is then given by:

$$heq(p_0, t) = h^*(p_0, -t) \otimes h(p_0, t) \quad (2)$$

While the equivalent impulse response of the unintended receiver is given by:

$$heq(p_{i, i \neq 0}, t) = h^*(p_0, -t) \otimes h(p_i, t) \quad (3)$$

SF is then evaluated as the ratio of the strongest peak power received by the intended receiver to the strongest peak received by the unintended receiver. The SF parameter can be written as:

$$SF_{[dB]} = 20 \log_{10} \left(\frac{\max(|heq(p_0, t)|)}{\max(|heq(p_1, t)|)} \right) \quad (4)$$

In a conventional railway environment, the use of a MISO 3×1 configuration is considered sufficient. We evaluated the contribution of TR in this configuration using the FG and SF. The study of SF and FG is performed for channel models exploiting the IEEE 802.15.3a channel model. This model is based on the Saleh Valenzuela formalism [8].

In the case of the IEEE 802.15.3a model, the characteristic values of Nakagami-m were explored, taking into account the number of antennas N_t .

Expression of the CIR is given by Eq. 5:

$$heq_{MISO}(t) = E \left\{ \sum_{i=1}^{N_t} heq_i(t) \right\} \quad (5)$$

where

$$heq_i(t) = \int_A \sum_{m=0}^{\infty} \alpha_{mi}^2 s_{mi}(\tau - t_{mi}) s_{mi}(\tau + t - t_{mi}) d\tau$$

Then,

$$\begin{aligned} heq_{MISO}(t) &= E \left\{ \int_A \sum_{i=1}^{N_t} \sum_{m=0}^{\infty} \alpha_{mi}^2 s_{mi}(\tau - t_{mi}) s_{mi}(\tau + t - t_{mi}) d\tau \right\} \\ heq_{MISO}(t) &= E \left\{ \sum_{i=1}^{N_t} \sum_{m=0}^{\infty} \alpha_{mi}^2 \right\} \Phi'_{si}(t) \\ heq_{MISO}(t) &= \sum_{i=1}^{N_t} \left[E \left\{ \sum_{m=0}^{\infty} \alpha_{mi}^2 \right\} \right] \Phi'_{si}(t) \end{aligned} \quad (6)$$

where $\Phi'_{si}(t) = \int_A s_i(\tau - t_i) s_i(\tau + t - t_i) d\tau$

The calculation of the average energy of the CIR in generic interval $W = [a, b]$ (a and b are arbitrary chosen) provides:

$$E \left\{ \sum_{i \in I_W} \alpha_i^2 \right\} = \int_W P_g(t) dt \quad (7)$$

where I_W is the random set containing the multipath components. The variance of the energy function of the CIR is given by:

$$\text{Var}\left\{\sum_{i \in I_W} \alpha_i^2\right\} = \int_W R_g(t) dt \quad (8)$$

where $R_g(t)$ is the kurtosis of the delay profile. Exploiting Eqs. (7) and (8), the expression $heq_{MISO}(t)$ becomes:

$$heq_{MISO}(t) = E_g \sum_{i=1}^{N_t} \Phi'_{si}(t) \quad (9)$$

The corresponding $(PDP_{ULB-RT}^{MISO}(t))$ is given by:

$$PDP_{TR-UWB}^{MISO}(t) = E\left\{\left|heq_{MISO}(t)\right|^2\right\} \quad (10)$$

After development, Eq. (10) becomes:

$$PDP_{TR-UWB}^{MISO}(t) = \sum_{i=1}^{N_t} \left\{ E_g^2 \Phi'_{si}(t) + \frac{E_g^2}{2\tau_{rms}} \varpi \right\}$$

where $\varpi = \left[\left(1 + \Psi_{\Phi'_{si}}(t)\right) c_{1i} \exp(-t/\tau_{rms}) + \left(1 + \frac{1}{m'}\right) 1\bar{\lambda} \Phi'_{si}(t) \right]$ and,

$$c_{1i} \Psi_{\Phi'_{si}}(t) = \int_{A'} \phi_s(\xi + t) \phi_s(\xi - t) d\xi d\tau,$$

$\Psi_{\Phi'_{si}}(t)$ is the normalised autocorrelation of $\Phi'_{si}(t)$ $\Psi_{\Phi'_{si}}(0) = 1$.

The corresponding focusing gain is given by Eq. (11):

$$FG_{[dB]} = 10 \log_{10} \left[\frac{E_g \sum_{i=1}^{N_t} \tau_{rms} + c_{1i} + c_2}{N_t} \right] \quad (11)$$

where $c_2 = \left(1 + \frac{1}{m'}\right) \frac{1}{2\lambda'}$, m' represents the Nakagami-m value.

The values obtained on the evaluation of focusing gain for MISO 3×1 configuration are presented in **Table 3**. These values correspond to the different IEEE 802.15.3a Channel Model configurations known as CM1, CM2 and CM3 corresponding to different increasing channel complexities. We obtain that changing from CM1 to CM3, FG increases from 14.6 to 20.1 dB. Therefore, as expected, the focusing gain increases, when the channel complexity increases.

IEEE 802.15.3a channel model	CM1	CM2	CM3
$FG_{\text{analytical}}$ [dB]	14.4	16.1	19.9
$FG_{\text{simulation}}$ [dB]	14.6	16.2	20.1

Table 3. FG in analytical and simulation study, case of MISO 3×1 (IEEE 802.15.3a channel model).

8.3. Contribution of TR-UWB system in terms of communication performance

UWB transmission optimised through Time-Reversal (TR) technique [8] is investigated and proved to be advantageous in multipath environments. This solution allows increasing the Signal-to-Noise Ratio (SNR) and therefore the communication range. This reduces interference effects and receiver complexity, improves data rates and multiuser capacity and provides Low Probability of Interception (LPI) to non-intentional users.

Under these assumptions, our simulations propose to demonstrate the benefit of UWB-TR transmission in the tunnel, especially in terms of ISI and MUI reduction, as well as providing higher throughputs at extended communication ranges. Both Single Input Single Output (SISO) and Multiple Input Single Output (MISO) transmissions were tested for both the conventional transmission mode (without TR) and the TR one. To consider and evaluate the performance of UWB-TR communication system in a very constraint railway environment, we introduced a channel model dedicated to tunnel environments. Moreover, to cope with this difficult environment, up to a MISO 4×1 is considered in this environment. We used a geometrical ray model simulating a tunnel. Based on geometric optics and the ray-tracing techniques, a straight 8 m wide and 6 m high, rectangular, infinite tunnel is simulated [8]. Uniform cross-section and lossy, smooth walls are assumed. Regarding this geometry and tunnel cross section, very large relative to our studied wavelengths (10 to 3 cm), this deterministic approach seems accurate and fast to implement and run. The model is exploited in the frequency domain, over the 3.1–10.6 GHz FCC2 authorised band. The transmitter is located at a particular place along the main axis of the tunnel, at different lateral positions (P1–P4), according to the parameter to estimate. The receiver moves along the main axis of the tunnel from a reference distance (1 m), then starting from 5 m up to a given distance noted d_n , using a 5-m step. The averaged and normalised power delay profile (PDP) are given in **Figure 6**. We evaluated temporal compression for three different Tx-Rx distances, $d = 5, 50$ and, finally, 100 m. Three scenarios have been tested: SISO without TR, SISO with TR and MISO-TR with four transmitting antennas ($NT_x = 4$). For SISO configurations, both Tx and Rx antennas were centred on the tunnel cross section. For MISO situations, as depicted in **Figure 7**, Rx antenna is centred, Tx antennas are positioned at the corners of a 50-cm square, one corner being the centre of the tunnel.

To evaluate the temporal focusing effectiveness, we computed the RMS (root-mean-square) delay spread using non-TR and TR configurations (see **Table 4**). As demonstrated in [14] for residential indoor environments case, the predicted delay spread in the tunnel environment for the SISO-TR case is not reduced. However, SISO-TR results in a highly peaked main lobe signal above the temporal side lobes. In the case of MISO-TR, temporal focusing is clearly improved. Results also show that using the highest number of transmitting antennas produces

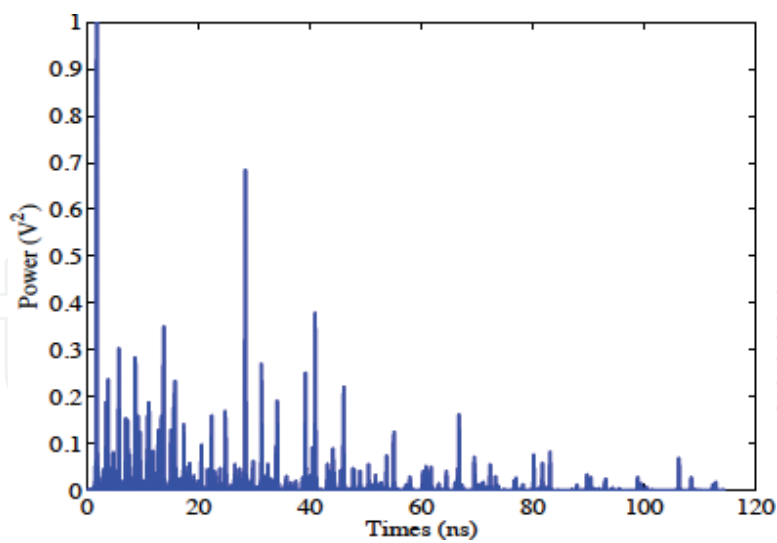


Figure 6. Averaged and normalised power delay profile (PDP).

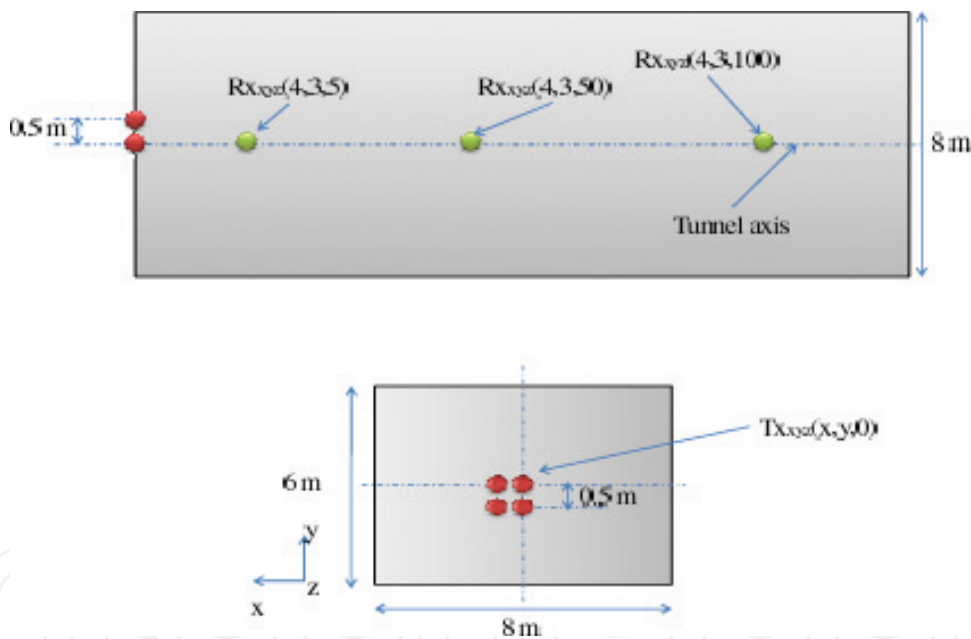


Figure 7. Time focusing simulation setup.

Distance	5 m	50 m	100 m
Without time reversal	31.55 ns	13.93 ns	8.20 ns
Time reversal SISO	32.55 ns	13.95 ns	8.42 ns
TR MISO NTx = 4	16.31 ns	10.62 ns	7.47 ns

Table 4. RMS delay spread comparison.

the better temporal compression, especially at the shortest Tx-Rx distances (by about a factor of 0.5). This can be explained by the scattering effect, more important at shortest distances than at farther distances. Consequently, the transmitter correlations are lower, resulting in a better temporal compression.

To evaluate the spatial focusing, two configurations were investigated for a Tx-Rx separation of $d = 5\text{ m}$: SISO-TR and MISO-TR (with $N_{Tx} = 2$). **Figure 8** illustrates power normalised to peak received in the area without TR. We observe that all users in this area receive approximately the same power level. This means that the communication can be intercepted by any receiver, and, in our case, the MUI problem can really affect the multiple access performance. By using TR (**Figure 9**), the power is decaying rapidly when moving away from the target area.

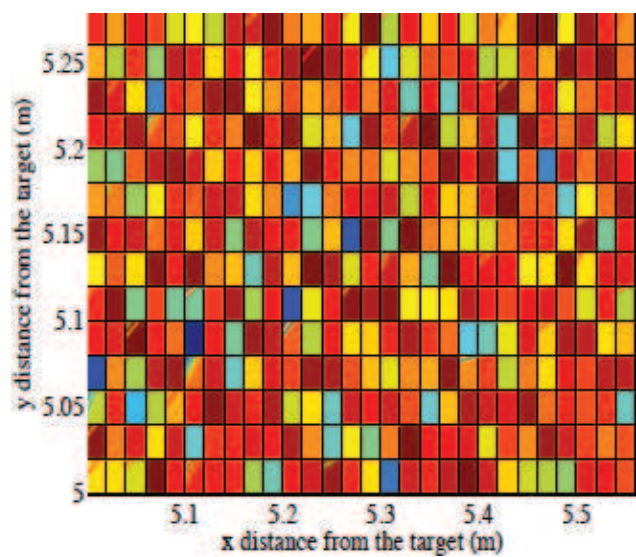


Figure 8. Power spatial repartition in the reception area.

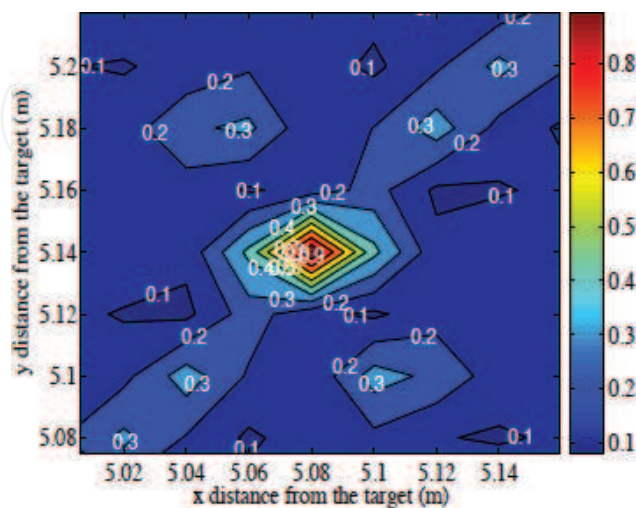


Figure 9. Spatial focusing gain in the SISO-TR case.

8.4. Contribution of TR-UWB system in terms of localization accuracy

The goal of this section is to estimate the contribution of TR in terms of precision of localization as a function of the propagation environment complexity. Using three base stations, we determine the position of a mobile in a 2D plane. To locate the mobile, each base station sends its own signal (recorded and reversed in time in the case of TR). As indicated before, the UWB-IR signals are built using the second-derivative Gaussian pulse. They are modulated by an antipodal modulation and coded by a Gold code, one code per base station. Processing is performed at the mobile (Rx) to determine its position relative to the base stations. The distance error is given by the difference between the calculated and the actual position of the mobile. The mobile receives the signals from each base station and performs an adequate signal processing to determine its position, relative to the base stations. Using the TDOA technique, the signal received at the mobile is processed to retrieve the position of the latter [19]. The Chan algorithm is used to solve the non-linear equations imposed by the TDOA technique. For the comparative study between the conventional localization system UWB-IR and the proposed TR_UWB system, we first use the UWB-IR case to locate the mobile, and then, the obtained information on the position of the mobile is used as reference for locating with the TR-UWB system. Our comparison is based on the computation of the Root Mean Square Error (RMSE) of localization between the conventional UWB-IR system and the proposed TR-UWB-IR system. We consider the IEEE 802.15.3a channel model (CM3). An AWGN is also injected into the channel. These results show that the combination of UWB and TR allows for a more accurate localization to be obtained that could be in line with the decimetre necessary level of precision required by the railway beacon application (**Figure 10**).

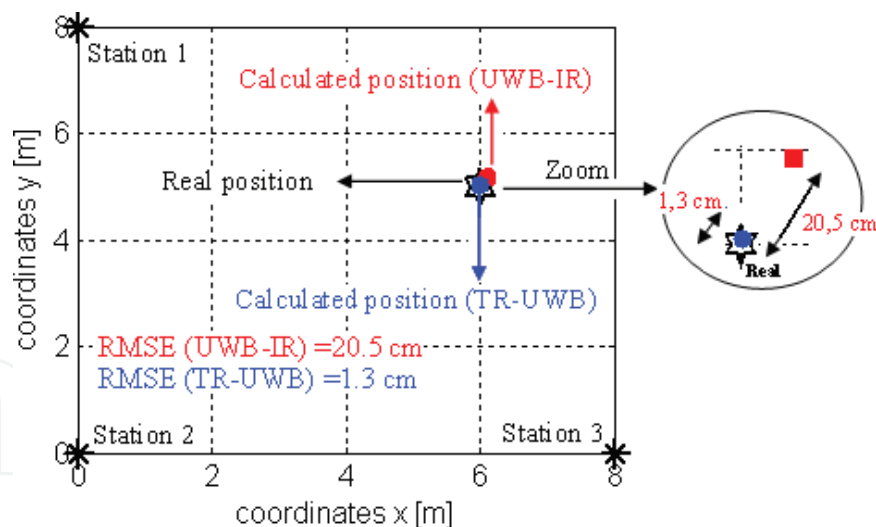


Figure 10. RMSE evaluation for conventional UWB-IR and TR-UWB (2D positioning system).

9. Experimental validation

The purpose of this experimental validation is to assess the impact of environmental complexity on performance related to temporal/spatial focusing and positioning error and to compare these conclusions to our preceding simulation results.

9.1. Experimental setup

An Arbitrary Waveform Generator (AWG) associated with a fast sampling oscilloscope (TDS) is used. The pulses generated by the AWG are radiated using wideband horn antennas. Similar antennas are used for receiving; their outputs are connected to the TDS ports through low noise amplifiers (LNAs). A portable computer is used to process the signals and store the results. The setup is installed in an anechoic chamber to control the radio channel. In this environment, metallic reflectors are introduced to create, on demand, different configurations of multipath. The dimensions of the anechoic chamber we used are $7 \times 7 \times 3$ m. It is operating from 100 MHz to 10 GHz. Two antenna cases are considered: SISO, MISO 3×1 cases. For each type of case, three configurations are considered: without addition of metal reflectors; a single aluminium plate ($2 \text{ m} \times 1 \text{ m}$) is introduced as a reflector between transmitters and receiver to generate a first multipath configuration; then, four plates are present to maximise the propagation environment complexity. The objective of these tests is to evaluate the focusing gain (FG), on the one hand, as the complexity of the propagation channel increases and, on the other hand, as the antenna configuration evolves from SISO to MISO 3×1 . For the SISO configuration, the distance between the transmitting antenna and the receiving antenna is set to 5 m, which is representative of an in-situ railway balise application. MISO 3×1 configuration corresponds to the addition of a third transmitting antenna located at a distance of 4 m between Tx3 and Rx. In a first step, for each selected configuration, a pulse is transmitted using the AWG; the received signal is acquired by the TDS and then returned temporally. In the cases of SISO and MISO 3×1 , each Tx re-emits its corresponding reversed in time signal. To assess this temporal focusing, we calculate the focusing gain (FG) obtained in each case. The overall results are grouped in **Table 5**. We obtain that, for each of the configuration, the focusing gain increases with the number of reflectors introduced. Moreover, by comparing the values of FG for these configurations, we find that FG increases from SISO to MISO configuration. To evaluate SF, we consider the scenario using three reflector plates. For the two SISO and MISO 3×1 configurations, the receiver is moved by 10 cm from its initial position. We note the initial position p_0 and p_1 and then the resulting ones after displacement. **Figure 11** represents an illustration of the SISO experimentation. The signal previously reversed in time at position p_0 is transmitted, and this signal is now received at position p_1 , where the used CSI is no more optimal. We then evaluate SF obtained at position p_0 , compared to SF obtained at position p_1 , using our two configurations and three reflector scenarios. The results are summarised in **Table 6**. We obtain that SF values increase with the number of reflectors but also as a function of the number of transmitting antennas. This confirms the results obtained in theory and verified by simulation (**Figure 12**).

Configuration	SISO	MISO 3×1
$FG_{\text{[dB]}}$ (without reflector)	1.0	1.7
$FG_{\text{[dB]}}$ (1 reflector plate)	2.2	5.9
$FG_{\text{[dB]}}$ (4 reflector plates)	6.1	12.8

Table 5. Focusing gain (FG) according to the number of reflector plates inserted in the propagation environment (case of SISO, and MISO 3×1 configurations).

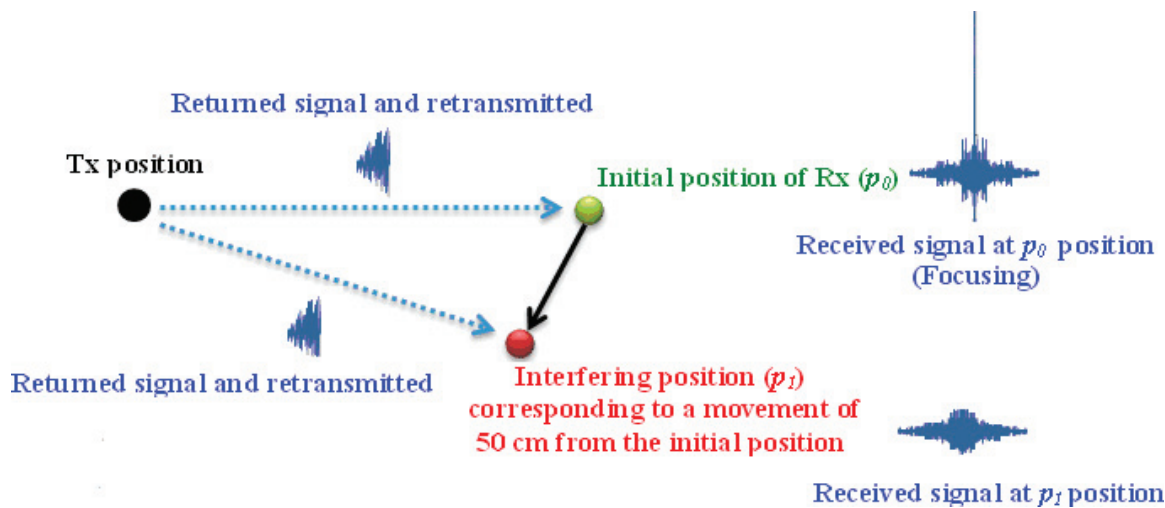


Figure 11. Principle of SF measurement.

Configuration	SISO	MISO 3 × 1
SF _[dB] (without reflector)	2.3	3.1
SF _[dB] (1 reflector plate)	5.8	8.1
SF _[dB] (4 reflector plates)	12.3	16.4

Table 6. SF according to the number of reflector plates inserted in the propagation environment.

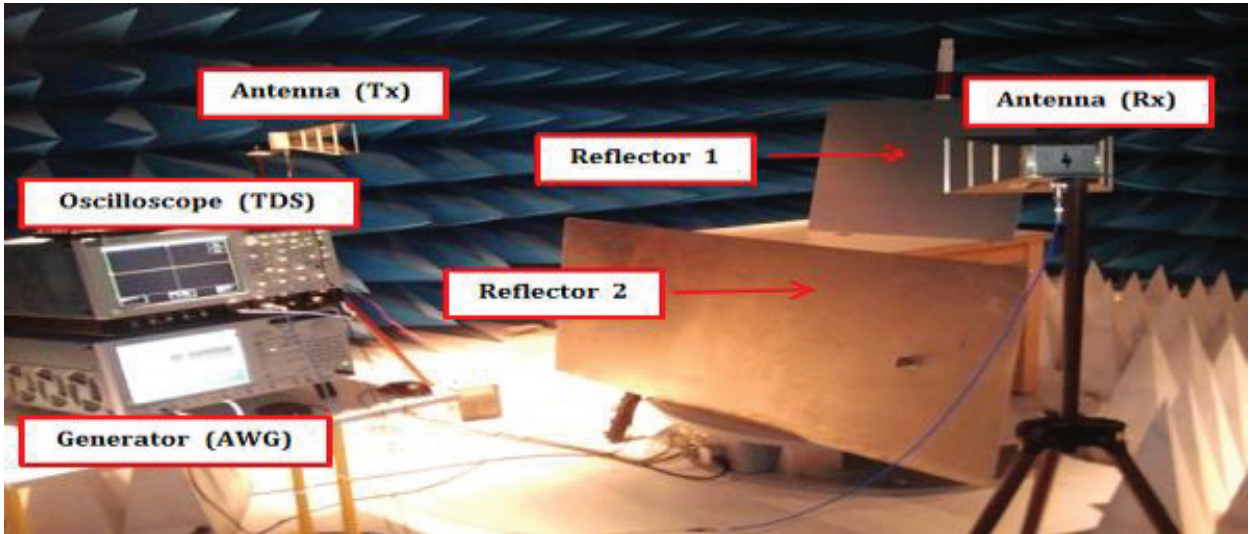


Figure 12. Implementation of the selected configurations (reflector plates in SISO).

9.2. Contribution of TR-UWB system in terms of communication performance

In the anechoic chamber, we considered five different reflector configurations. Three series of acquisition were performed. In each case, a sequence of seven pulses is sent. After processing, we determine the position of the mobile. Figure 13 shows the corresponding position errors.

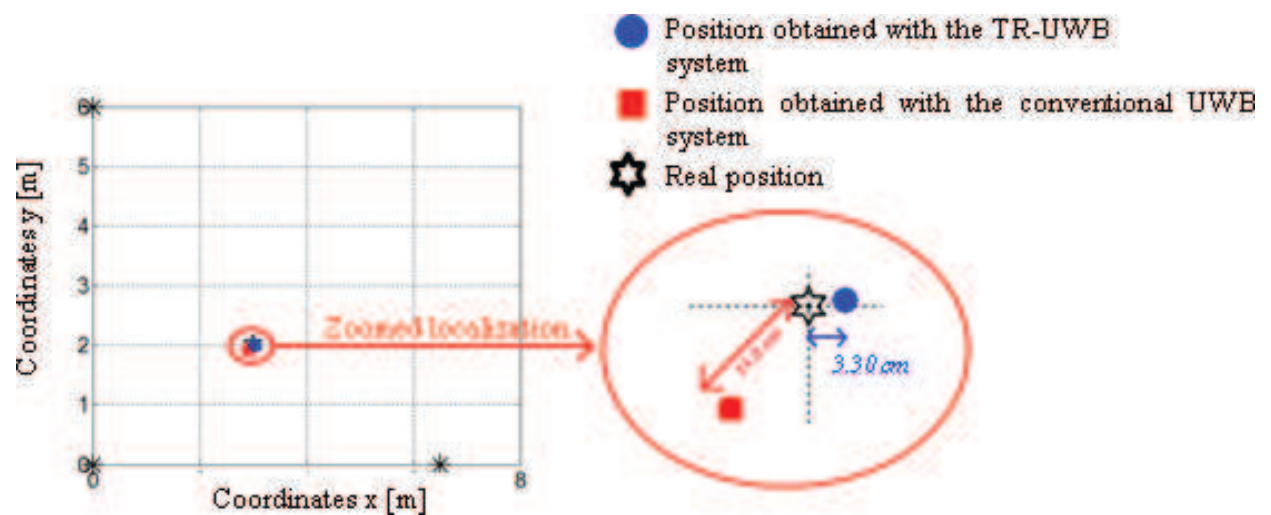


Figure 13. Conventional UWB and TR-UWB localization systems (scenario with three reflector plates in an anechoic chamber).



Figure 14. Implementation of tests configuration.

With the conventional UWB localization system, we get an error of 11.0 cm, decreasing to 3.3 cm in the case of TR-UWB (**Figure 14**).

10. Conclusion

As mentioned in Section 3, railway beacons are safety critical pieces of equipment. Therefore, a final industrial product will have to comply with SIL 4 requirements. To achieve this high level of integrity, one major goal consists in demonstrating that no single failure of this piece of equipment would lead to a railway safety critical situation. For such a demonstration, let us

examine the advantages that are provided by the proposed association of UWB and time reversal techniques. The UWB radio technique alone already provides some interesting advantages that will intrinsically facilitate a future SIL 4 demonstration. First, an UWB-IR radio transmitter contains a limited number of components. Therefore, a safety demonstration will be easier to be realised than for a more sophisticated conventional radio transmitter. Complementary major advantages related to the use of the UWB technique are its high throughput capacity due to its wide frequency range and its availability and robustness to multiple paths, thanks to the large occupied bandwidth. The coexistence of the UWB signals with other radio systems due to the low involved power spectral densities is also interesting to note; this usually implies that there is need for a dedicated frequency allocation. Moreover, in a railway environment characterised by large radio interference, the intrinsic resistance of UWB signals to narrow band or even wide band radio interference is also very beneficial. Finally, due to its low power and large spectrum used, the low probability of interception of UWB transmitted signals by non-accredited users is also quite interesting. Indeed, this property will be in more demand for a secure operation of the transport system. As demonstrated in the previous sections, coupling the time reversal precoding technique to the UWB radio technique also improves some of these initial advantages in terms of higher throughput, accuracy of location etc. Moreover, since a MISO radio scheme is used, the failure of one transmitter among the different ones used for time reversal will reduce the spatial and temporal focalisation levels of performance, but the critical radio link with the train will still be maintained. Concerning jamming, spoofing and meaconing attacks that are becoming more critical in satellite systems, civil location and time assurance, spatial focusing delivers significant improvements. Indeed if valid beacon signals can only be received in a very limited zone or time window while the train is running, this property can be used to reject signals that are coming from non-valid distant transmitters, which do not present these focusing characteristics.

Acknowledgements

This present research work has been supported by SAFER-LC H2020 European Project, InterCor Project and ELSAT 2020. ELSAT 2020 project is co-financed by the European Union with the European Regional Development Fund, the French state and the Hauts de France Region Council.

Author details

Fouzia Elbahhar^{1,2*} and Marc Heddebaut^{1,2}

*Address all correspondence to: fouzia.boukour@ifsttar.fr

1 Univ. Lille Nord de France, Lille, France

2 IFSTTAR, LEOST, Villeneuve d'Ascq, France

References

- [1] Kirkwood D, Tibbs B. Developments in SIL determination. *IET Computing & Control Engineering Journal*. June-July 2005;**16**(3):21-27
- [2] Frederic Howard L. Track-circuit signaling on electrified roads. *Proceedings of the American Institute of Electrical Engineers*. Aug 1907;**26**(8):1277-1292
- [3] Hill RJ. Optimal construction of synchronizable coding for railway track circuit data transmission. *IEEE Transactions on Vehicular Technology*; **39**(4):390-399
- [4] Ogunsola A, Mariscotti A. *Electromagnetic Compatibility in Railways: Analysis and Management*, Lecture Notes in Electrical Engineering. Verlag Berlin Heidelberg: Ed. Springer; 2013. pp. 119-125
- [5] Transportation Research Board (TRB). *Track Design Handbook for Light Rail Transit*, TCRP 105. 2nd ed. pp. 10-11
- [6] Zhang X, Tentzeris M. Applications of fast-moving RFID tags in high-speed railway systems. *International Journal of Engineering Business Management*. 2011;**3**(1):27-31
- [7] FFIIS for Eurobalise, subset-036, issue 3.0, February 24, 2012. Available on the Internet, <http://www.era.europa.eu/Document-Register/Documents/Set-2-Index009-SUBSET-036%20v300.pdf>
- [8] Saghir H, Heddebaut M, Elbahhar F, Rouvaen JM, Rivenq A, Ghys JP. Train-to-wayside wireless communication in tunnel using ultra-wideband and time reversal. *Transportation Research, Part C: Emerging Technologies*. 2009;**17**(1):81-97
- [9] Lerosey G, de Rosny J, Tourin A, Derode A, Montaldo G, Fink M. Time reversal of electromagnetic waves and telecommunication, 17 September 2005. *Radio Science*. December 2005;**40**(6):1
- [10] Molish AF. Ultrawideband propagation channel-theory, measurement, and modelling. *IEEE Transactions on Vehicular Technology*. 2005;**54**(5):1528-1545
- [11] Porcino D, Hirt W. Ultra-wideband radio technology: Potential and challenges ahead. *IEEE Communications Magazine*. Juillet 2003;**41**(7):66-74
- [12] Suwansantisuk W, Win MZ, Shepp LA. On the performance of wide-bandwidth signal acquisition in dense multipath channels. *IEEE Transactions on Vehicular Technology*. Sept. 2005;**54**(5):1584-1594
- [13] Strohmer T, Emami M, Hansen J, Papanicolaou G, Paulraj A. Application of time-reversal with MMSE equalizer to UWB communications. *Proceedings of Globecom Conference*, Dallas. 2004. pp. 3123-3127
- [14] Fall B, Elbahhar F, Heddebaut M, Rivenq A. Time-reversal UWB positioning beacon for railway application. *International Conference on Indoor Positioning and Indoor Navigation (IPIN)*. 2012

- [15] Bouna Fall, Fouzia Elbahhar, Marc Heddebaut, Atika Rivenq, Maria-Gabriella Di Benedetto: Assessment of the contribution of time reversal on a UWB localization system for railway applications. *International Journal of Intelligent Transportation Systems Research*. 2016;14(3): 139-151
- [16] Fink M. Time reversal waves and super resolution. *Journal of Physics. Conference series* 124. 4th AIP international conference and the 1st congress of the IPIA. 2008
- [17] Liu X, Wang B-Z, Xiao S, Deng J. Performance of impulse radio UWB communication based on time reversal technique. *Progress in Electromagnetics Research*. 2008;79(11):401-413
- [18] Abassi-Moghadam D, TabatabaVakili D. Channel characterization of time reversal UWB communication systems. *International Journal of Communication Systems*. 2010;65(9–10): 601-614
- [19] Ghavami M, Michael LV, Kohno R. *Ultra Wide Band Signals and Systems in Communication Engineering*. Wiley. London, 2007, 247 p

